



## Variable angle NMR spectroscopy and its application to the measurement of residual chemical shift anisotropy

Grit Kummerlöwe<sup>a,b</sup>, Stephan L. Grage<sup>b</sup>, Christina M. Thiele<sup>c</sup>, Ilya Kuprov<sup>d</sup>, Anne S. Ulrich<sup>b,e</sup>, Burkhard Luy<sup>a,b,e,\*</sup>

<sup>a</sup> Department Chemie, Lehrstuhl Organische Chemie II, Technische Universität München, Lichtenbergstraße 4, D-85747 Garching, Germany

<sup>b</sup> Institut für Biologische Grenzflächen (IBG-2), Karlsruher Institut für Technologie, Postfach 3640, 76021 Karlsruhe, Germany

<sup>c</sup> Technische Universität Darmstadt, Clemens-Schöpf-Institut für Organische Chemie und Biochemie, Petersenstraße 22, D-64287 Darmstadt, Germany

<sup>d</sup> Oxford e-Research Centre, University of Oxford, 7 Keble Road, Oxford OX1 3QG, UK

<sup>e</sup> Institut für Organische Chemie, Karlsruher Institut für Technologie, Fritz-Haber-Weg 6, 76131 Karlsruhe, Germany

### ARTICLE INFO

#### Article history:

Received 27 August 2010

Revised 30 November 2010

Available online 16 December 2010

#### Keywords:

Variable angle NMR

Alignment

Scaling

Residual chemical shift anisotropy

Chemical shift reference

Magic angle

### ABSTRACT

The successful measurement of anisotropic NMR parameters like residual dipolar couplings (RDCs), residual quadrupolar couplings (RQCs), or residual chemical shift anisotropy (RCSA) involves the partial alignment of solute molecules in an alignment medium. To avoid any influence of the change of environment from the isotropic to the anisotropic sample, the measurement of both datasets with a single sample is highly desirable. Here, we introduce the scaling of alignment for mechanically stretched polymer gels by varying the angle of the director of alignment relative to the static magnetic field, which we call variable angle NMR spectroscopy (VA-NMR). The technique is closely related to variable angle sample spinning NMR spectroscopy (VASS-NMR) of liquid crystalline samples, but due to the mechanical fixation of the director of alignment no sample spinning is necessary. Also, in contrast to VASS-NMR, VA-NMR works for the full range of sample inclinations between 0° and 90°. Isotropic spectra are obtained at the magic angle. As a demonstration of the approach we measure <sup>13</sup>C-RCSA values for strychnine in a stretched PDMS/CDCl<sub>3</sub> gel and show their usefulness for assignment purposes. In this context special care has been taken with respect to the exact calibration of chemical shift data, for which three approaches have been derived and tested.

© 2010 Elsevier Inc. All rights reserved.

### 1. Introduction

In recent years NMR spectroscopy on partially oriented samples has significantly extended the possibilities for structure determination of small molecules [1–4]. The numerous applications range from improved assignment [5,6], discrimination of enantiomers [7–15], the indirect measurement of J-couplings [16], enhanced resolution by RDCs [17], relative configuration [18–29], and the 3D-conformation of molecules [30–36]. Next to liquid crystalline alignment media [37,38], the full power in structure determination is reached by stretched gels, which are now available for the major NMR solvents [21,26,39–47], with no lower limit in alignment strength.

Residual anisotropic interactions like residual dipolar couplings (RDCs), residual quadrupolar couplings (RQCs), and residual chemical shift anisotropies (RCSAs) are usually extracted as the difference of couplings or chemical shift values measured in a

conventional liquid sample and in a separate sample with the appropriate alignment medium. This method has the disadvantage that the molecule of interest is measured in two different chemical environments in which the isotropic NMR quantities might differ significantly [48], even up to the point where the assignment has to be repeated for the aligned sample [49]. This difference can also appear when the sample undergoes a first order phase transition, as, e.g., for samples measured in bicelle phases below and above the corresponding transition temperature to the lyotropic mesophase. The reliability of measured anisotropic interactions would be improved significantly if all measurements were carried out in the same sample as has been shown exemplarily before [50,51]. For the measurement of RCSA values it is also important to have a reliable referencing of chemical shift values.

In this article, we present a method for measuring anisotropic NMR parameters in a single sample by changing the angle of the director of alignment (in this case the stretching axis of a mechanically stretched polymer gel) with respect to the static magnetic field. After an introduction to the approach and a short comparison with other scaling techniques, its application to the measurement of residual chemical shift anisotropy within a single stretched

\* Corresponding author at: Institut für Biologische Grenzflächen (IBG-2), Karlsruher Institut für Technologie, Postfach 3640, 76021 Karlsruhe, Germany.

E-mail address: [Burkhard.Luy@kit.edu](mailto:Burkhard.Luy@kit.edu) (B. Luy).

PDMS/ $\text{CDCl}_3$  gel is examined in detail. In this context, special care has been taken to compensate for RCSA effects of the chemical shift reference tetramethylsilane (TMS) based on one theoretically derived and two empirical approaches.

## 2. Variable angle NMR (VA-NMR)

Already as early as 1964 A. Saupe pointed out that the magnitude and sign of anisotropic interactions in a liquid crystalline phase can be scaled by changing the angle  $\Theta$  of the director of the mesophase relative to the static magnetic field  $B_0$  [52]. In this case, the magnitude of observed anisotropic parameters is scaled according to  $\frac{3}{2} \cos^2 \Theta - \frac{1}{2}$ . The same relation is valid for alignment induced by stretched gels, for which the angle of the stretching axis relative to  $B_0$  then has to be varied. There are several ways of changing the angle  $\Theta$  of a stretched gel with respect to the external field.

One possibility, for example, could utilize an unstretched gel with a non-cylindrical shape that would swell within a conventional NMR tube along an axis non-parallel to the magnetic field. This approach, however, would be difficult to control. We therefore decided to use a more straightforward approach based on available solid state NMR hardware, for which a uniaxial, cylindrically symmetric stretching of the sample is sufficient. Tilting of the sample is achieved within a variable angle sample spinning (VASS) probehead or a combination of a magic angle sample spinning (MAS) and a conventional liquid state probehead.

### 2.1. Sample preparation

For our studies, we used a 5 mm 500 MHz HFX4 4-channel VASS probehead (Doty Scientific, Columbia, SC) and a 4 mm 500 MHz HCX 3-channel MAS probehead (Bruker, Rheinstetten, Germany). The sample containers specifically designed for these probeheads are 5 mm and 4 mm zirconia rotors, respectively. Our initial studies therefore focussed on these rotors (see Fig. 1a). The preparation of stretched gels in the rotors is equivalent to the preparation in conventional NMR tubes as previously described for PS and PDMS [21,43]: a dry crosslinked polymer stick is placed into the rotor, and solvent is added. The stick then swells and stretches itself as soon as it reaches the walls of the rotor. The only practical difference of swelling the gel in a rotor compared to swelling it in an

NMR tube is the length of the gel cylinder to be considered. As in the optimum case the whole rotor should be filled by the gel, it easily can happen that the gel protrudes from the rotor after swelling, if the stick dimensions have been chosen too large. In this case the top of the gel simply can be cut back with a scalpel after equilibration. The dissolved solute molecules can either be put in contact with the top of the rotor after equilibration for diffusion, or they can be added together with the solvent for swelling. For 5 mm rotors the polymer stick diameters are identical to the values reported for a 5 mm NMR tube [11,21,26,43,44,46,48], while slightly reduced diameters have to be used for 4 mm rotors.

As no sample spinning and therefore no expensive rotor is required for measuring anisotropic parameters, we also explored cost-saving sample preparations. After a number of trials, we found useful variants of preparation, as shown in Fig. 1b and c: first, a conventional NMR tube of 5 or 4 mm diameter is cut to pieces of roughly 3–4 cm length; then the polymer stick is cut to the appropriate length and placed either at the bottom of the closed part of the end-piece of the NMR tube (Fig. 1) or in the center of a glass tube with two open ends (Fig. 1) and put into the solvent for swelling and stretching; finally, after addition of the solute, the open ends of the samples are sealed either by an appropriate plug (in our case we melted poly(ethylene) with a molecular weight of 35,000 to the appropriate shape) or by filling the hole with epoxide based glue (UHU plus endfest 300, UHU GmbH & Co. KG, Bühl, Germany). In the case of  $\text{CDCl}_3$  as the solvent, layers of  $\text{D}_2\text{O}$  were added between the polymer gel and the sealing, as the solvent induces unwanted swelling of the plug and glue.

For the measurements presented in this article, 5 and 4 mm rotors and a 4 mm glass tube were used. The 5 mm rotor was filled with a PU/ $\text{CDCl}_3$  gel made from a 3.2 mm dry PU-stick crosslinked with 120 kGy of accelerated electrons (a manuscript with detailed characterization of polyurethanes (PU) as alignment media is in preparation). For the measurements of strychnine RCSA values various identical samples were prepared with PDMS sticks of 5 mm length and 3 mm diameter (ABCR GmbH and Co.KG, Karlsruhe, Germany, DMS-T61; 1000000 cSt., irradiated with 480 kGy of accelerated electrons [21]). The sticks were directly swollen using a solution of 0.06 g/mL strychnine in  $\text{CDCl}_3$  and  $\approx 5\%$  TMS inside a 4 mm rotor or in 4 mm glass tubes. The gels were incubated two weeks in the solution for equilibration.

### 2.2. Angular dependence of alignment strength

Our first goal was to prove that the relationship between the size of anisotropic parameters and the angle to the magnetic field as derived by A. Saupe for liquid crystals [52] also holds for stretched gels. For this purpose we used a probehead designed for variable angle sample spinning NMR (VASS-NMR, [50,51,53]). The commercially available probehead (500 MHz HFX4 4-channel VASS probehead with two crossed Helmholtz coils for  $^1\text{H}$  and  $^{19}\text{F}$ , and solenoid coil for X and Y, Doty Scientific, Columbia, SC) is designed such that rf-irradiation always has a component perpendicular to the  $B_0$  field for all angles  $\Theta$  of the sample axis with respect to the external field. By varying the angle  $\Theta$ , as shown in Fig. 2a, the  $\frac{3}{2} \cos^2 \Theta - \frac{1}{2}$  dependence should be observable for any anisotropic NMR parameter.

The values of the deuterium quadrupolar splitting  $|\Delta\nu_Q|$  of  $\text{CDCl}_3$  from simple  $^2\text{H}$ -1D experiments are shown in Fig. 2b. Clearly the collapse of the residual quadrupolar coupling at the magic angle ( $54.7^\circ$ ) is visible and the size of the splittings can nicely be fitted by the absolute value  $|\frac{3}{2} \cos^2 \Theta - \frac{1}{2}|$  with a constant scaling factor.

Although we could validate our concept for the full range of  $\Theta$  angles ( $0$ – $90^\circ$ ), the experimental setup with the available VASS probehead had several disadvantages for real applications, as the

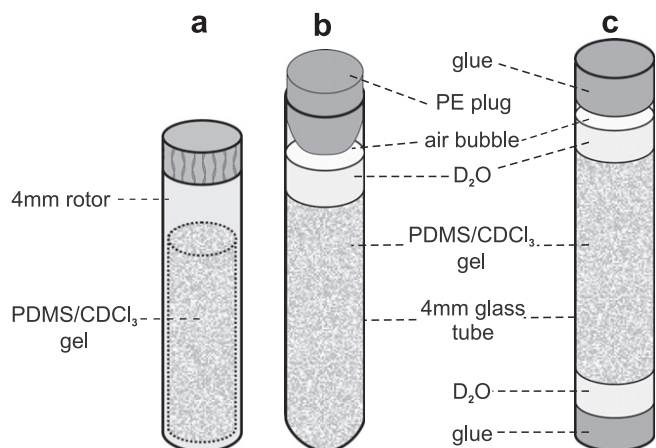


**Fig. 1.** Sample preparation for VA-NMR. (a) The corresponding gel is swollen and stretched inside a conventional MAS-rotor. (b and c) A cheaper alternative is the preparation in a cut NMR tube. After swelling and stretching of the gel, the bottom (b) or intermediate part (c) of an NMR tube is sealed at the open ends by either a poly(ethylene) plug (b) or epoxide glue (c). When using nonpolar organic solvents like  $\text{CDCl}_3$ , swelling of poly(ethylene) and epoxide, respectively, is prevented by an additional layer of  $\text{D}_2\text{O}$ .

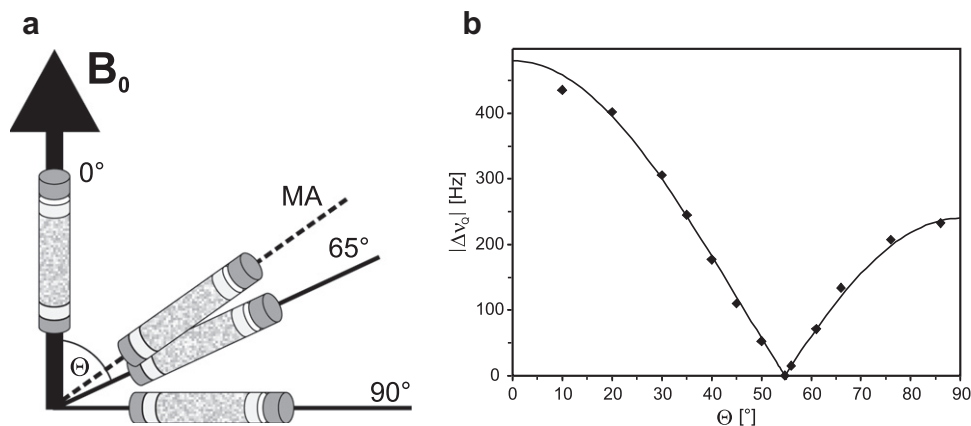


**Fig. 2.** Concept of VA-NMR. (a) By varying the angle  $\Theta$  of the director of the mechanically stretched gel relative to the static  $B_0$  field anisotropic NMR parameters can be scaled over the entire possible range without the need of sample spinning (MA: magic angle at  $54.7^\circ$ ). (b) The quadrupolar splitting  $|\Delta\nu_Q|$  of  $\text{CDCl}_3$  measured at various angles  $\Theta$  follows the expected scaling  $|3\cos^2\Theta - 1|$ .

probehead showed low sensitivity in  $^{13}\text{C}$  direct detection and could not be shimmed anywhere close to high resolution linewidths. To improve the situation with the NMR equipment accessible to us we therefore switched to a different approach with a 4 mm Bruker MAS probehead where we could achieve reasonable  $^{13}\text{C}$  linewidths of  $\approx 25$  Hz (at the magic angle) and  $\approx 50$  Hz (at  $\Theta = 65^\circ$ ) and relatively good sensitivity. The accessible angular range of the MAS probehead, however, was limited to approximately  $45\text{--}65^\circ$ . A compromise for measuring at least one more angle with  $\Theta \approx 0^\circ$  and sufficient sensitivity was then to use a liquid state probehead (Bruker 500 MHz TXI  $^1\text{H}$ ,  $^{13}\text{C}$ ,  $^{15}\text{N}$ -triple resonance, optimized for proton detection). In this case, the 4 mm rotor or glass tube was simply placed into a conventional 5 mm NMR tube for straightforward acquisition of high resolution spectra with a linewidth of approximately 8 Hz.

### 2.3. Comparison of VA-NMR with other scaling techniques

Besides variable angle NMR on stretched polymer gels as proposed here, there are two other effective techniques for scaling the alignment strength in a single weakly aligned sample: variable angle sample spinning (VASS-NMR) with liquid crystalline phases [50,51,53], and a rubber-based stretching apparatus for stretched gels with polar [14,58–60] and apolar solvents [61].

VA-NMR is obviously related to VASS-NMR. In both cases scaling of NMR parameters is achieved by tilting the sample relative to the static  $B_0$  field. However, in VASS-NMR certain conditions have to be fulfilled to achieve alignment along the rotor axis with a liquid crystalline alignment medium. On the one hand, the spinning speed has to be above a certain threshold frequency determined by the square of the magnetic field  $B_0^2$  and a so-called rotational viscosity coefficient [50]. On the other hand it has to be below a frequency given by the inertial torque of most commonly used mesophases with relatively low magnetic susceptibility anisotropy [50]. The resulting spinning speeds of several hundred Hertz may lead to spinning side bands.

In addition, the range of accessible angles is limited for VASS-NMR. Liquid crystals with a positive magnetic susceptibility anisotropy allow stable orientation of the director along the spinning axis for angles  $0^\circ \leq \Theta < 54.7^\circ$ , while mesophases with negative magnetic susceptibility anisotropy result in stable orientation for  $54.7^\circ < \Theta \leq 90^\circ$  [50]. For the respective other angular range, sample spinning leads to orientation of the director perpendicular to the spinning axis with highly modulated spectra. Only in rare cases, as for example with the addition of lanthanide ions to

phospholipid bicelles [55–57], the magnetic susceptibility anisotropy can be reversed for a wider range of angles. At the magic angle itself the orientation of the director is always metastable between both solutions.

None of these limitations apply to VA-NMR with stretched gels. As the induced order and therefore the director of alignment is determined by mechanical stretching, the sample can be aligned at any angle  $\Theta$  without sample spinning. Accordingly, the resulting spectra can be fully scaled with respect to the anisotropic parameter strength and do not suffer from spinning sidebands.

The silicone-rubber-based stretching apparatus introduced by Kuchel et al. [58] allows the scaling of alignment by stretching a polymer gel inside a rubber tubing. The main advantage of this approach is that conventional liquid state NMR equipment with its high shimming quality and optimal sensitivity can be used, and due to the stretching inside the rubber tube no change in polymer concentration is observed. However, covalently crosslinked polymer gels can only be stretched, which is equivalent to the angular variation of  $\Theta$  between  $0^\circ$  and  $54.7^\circ$  in the VA-NMR approach. Only for special cases like gelatin as an alignment medium with H-bond based crosslinking that can be melted at temperatures above  $35^\circ\text{C}$ , also a compression with the rubber tube is possible [14,59], equivalent to the full range of  $\Theta$ . Another disadvantage of the silicone rubber tube is the limited applicability with respect to NMR solvents. Samples based on  $\text{CDCl}_3$  as used here, for example, are not compatible with the silicone tubing and the approach cannot be applied. A promising but significantly more expensive and more difficult to manufacture stretching device for also nonpolar solvents has recently been developed [61]. We conclude that the stretching apparatus in principle has a number of advantages concerning achievable linewidth and sensitivity, but, in contrast to VA-NMR, its applicability with respect to the scaling of alignment and potential solvents appears to be limited, though the solvent incompatibilities may be overcome by the newly developed stretching device.

A third method for scaling the alignment is based on the use of Shigemi plungers for compressing gels or restricting their ability to stretch, as has been introduced previously for poly(acrylamide) gels [39], and in a nice publication by the Gil group for poly(methyl methacrylate) gels [62]. This approach is easy to apply, leads to alignment equivalent to the full range of angles  $\Theta$ , and does not require any special equipment. However, a change of alignment in this case is combined with a change of concentration of the polymer, since some solvent is always removed or added to the gel. As will be seen in following sections this might have a profound

effect on the chemical shifts of solute and reference signals and can therefore not be used for the reliable determination of RCSA values. The measurement of RDCs, instead, should not be affected.

### 3. Practical aspects of chemical shift measurement

In principle, chemical shifts are easily measured, as the corresponding frequency value can simply be read off as the center of a given multiplet. When measuring RCSA values, however, highest accuracy in determining the frequency is essential, as the observed changes in chemical shifts upon alignment are only tens of ppb's even for aromatic carbons, and various contributions from different sources may influence the results. Before going to a case study of measuring RCSA values with the VA-NMR approach, we would thus like to provide a detailed view of chemical shift referencing in partially aligned samples.

#### 3.1. Theory

All measurements of RCSA contain a contribution from bulk and intermolecular effects. The magnetic field experienced at the site of a particular nucleus depends, e.g., on the overall magnetic susceptibility and shape of the bulk sample [63], and can be summarized in the chemical shift contribution  $\sigma_{\text{bulk}}$  [64]. This bulk effect can be on the order of or even larger than the actual chemical shifts due to chemical shielding, and it can only be neglected when an internal reference with identical bulk properties is used for measurement. In addition, intermolecular effects from neighboring molecules have to be considered. For example, significant chemical shift changes can be caused by changing the solvent. Not only the kind of molecules surrounding the solute of interest is important, but also its phase state. E.g., liquid crystals typically show a distinct chemical shift jump when the temperature is changed through the first order phase transition from the isotropic to the liquid crystalline phase [65]. The effect of the local intermolecular interactions on the chemical shift can be summarized as  $\sigma_{\text{local}}$ . With the chemical shift contribution of the molecule itself,  $\sigma_{\text{mol}}$ , an experimental chemical shift measurement in an isotropic environment can then be described by [65]

$$\sigma^{\text{iso}} = \sigma_{\text{local}} + \sigma_{\text{mol}} + \sigma_{\text{bulk}}. \quad (1)$$

If the molecule of interest is brought into an aligned phase, additional contributions to the chemical shifts due to changes in susceptibility and a potentially changed shape of the overall sample ( $\Delta\sigma_{\text{bulk}}$ ), differing local environments ( $\Delta\sigma_{\text{local}}$ ) and, finally, due to the chemical shift anisotropy of the molecule itself ( $\Delta\sigma_{\text{mol}}$ ) must be considered. The resulting measured chemical shift can then be expressed by the sum

$$\sigma^{\text{aniso}} = \sigma_{\text{local}} + \Delta\sigma_{\text{local}} + \sigma_{\text{mol}} + \Delta\sigma_{\text{mol}} + \sigma_{\text{bulk}} + \Delta\sigma_{\text{bulk}}. \quad (2)$$

The difference of chemical shift values between a partially aligned and an isotropic sample thus results in

$$\Delta\sigma = \sigma^{\text{aniso}} - \sigma^{\text{iso}} = \Delta\sigma_{\text{local}} + \Delta\sigma_{\text{mol}} + \Delta\sigma_{\text{bulk}}. \quad (3)$$

The quantity which corresponds to the desired RCSA value, however, is only the molecular contribution  $\Delta\sigma_{\text{mol}}$  and not the overall change in chemical shift  $\Delta\sigma$ . Examples which do not take into account this well-known relation unfortunately can be found frequently in the literature. As pointed out before, it also affects measurements that are performed in a single sample but at two different temperatures below and above the liquid crystalline phase transition. Even if the temperature coefficients of the chemical shifts are known, the first order phase transition will result in an abrupt jump in  $\Delta\sigma_{\text{local}}$  that cannot be taken care of adequately.

While Eqs. (1)–(3) describe the situation of chemical shift measurement without or with only an external chemical shift reference, an internal chemical shift reference improves the situation. With the chemical shift of the reference signal  $\sigma^{\text{iso},0} = \sigma_{\text{local}}^0 + \sigma_{\text{mol}}^0 + \sigma_{\text{bulk}}^0$  the measured isotropic chemical shift corresponds to

$$\begin{aligned} \sigma^{\text{iso}} &= \sigma_{\text{local}} + \sigma_{\text{mol}} + \sigma_{\text{bulk}} - \sigma_{\text{local}}^0 - \sigma_{\text{mol}}^0 - \sigma_{\text{bulk}}^0 \\ &= \sigma_{\text{mol}} + \sigma_{\text{local}} - \sigma_{\text{mol}}^0. \end{aligned} \quad (4)$$

This expression takes into account that sample shape and susceptibility for the solute molecule and the internal reference are identical ( $\sigma_{\text{bulk}} = \sigma_{\text{bulk}}^0$ ), and that an internal reference like tetramethylsilane (TMS) is usually chosen in a way that its chemical shift does not depend on its local environment ( $\sigma_{\text{local}}^0 \approx 0$ ). The situation of Eq. (4) applies to isotropic samples as well as the VA-NMR approach at the magic angle. The corresponding measurement in an anisotropic environment or at a different angle  $\Theta$  leads to

$$\sigma^{\text{aniso}} = \sigma_{\text{local}} + \Delta\sigma_{\text{local}} + \sigma_{\text{mol}} + \Delta\sigma_{\text{mol}} - \sigma_{\text{mol}}^0 - \Delta\sigma_{\text{mol}}^0, \quad (5)$$

and the measured chemical shift difference results in

$$\Delta\sigma = \Delta\sigma_{\text{local}} + \Delta\sigma_{\text{mol}} - \Delta\sigma_{\text{mol}}^0. \quad (6)$$

With the internal chemical shift reference we are therefore able to eliminate the bulk chemical shift contribution, but also introduce the RCSA of the internal reference ( $\Delta\sigma_{\text{mol}}^0$ ) as an additional factor to be considered. Looking at Eq. (6), VA-NMR with the advantage of performing all measurements in a single sample becomes important, as the local environment remains unchanged and  $\Delta\sigma_{\text{local}}$  will be negligible. The difference of two chemical shift measurements in identical samples but at different angles  $\Theta$  thus can be described by

$$\Delta\sigma^{\text{VA}} = \Delta\sigma_{\text{mol}} - \Delta\sigma_{\text{mol}}^0, \quad (7)$$

which leaves the desired RCSA value of the solute molecule minus the RCSA value of the internal reference. It is therefore necessary to know  $\Delta\sigma_{\text{mol}}^0$  to obtain accurate RCSA data for the solute.

#### 3.2. Residual chemical shift anisotropy of the internal reference

As mentioned before, chemical shift reference compounds are usually chosen to be affected as little as possible by changes of solvents or solute molecules. This can usually be correlated to a very small inherent chemical shift anisotropy. TMS, for example, has tetrahedral symmetry which at first sight would imply a vanishing CSA tensor. In this case,  $\Delta\sigma_{\text{mol}}^0$  should be zero and RCSA values would most easily be obtained. However, residual dipolar couplings and chemical shift anisotropies have been reported for tetrahedral molecules in ordered media due to vibration-reorientation interactions [66–69]. In essence, measurable anisotropic NMR parameters are always observed when the orientational averaging of the tetrahedral molecule occurs on a similar time scale as corresponding vibrational motions.

As TMS possesses four methyl groups which *per se* have a very low CSA, we were hopeful that  $\Delta\sigma_{\text{mol}}^0$  would be negligibly small. In order to assess this assumption, we measured RDCs on TMS and the chemical shift difference of the two tetrahedral molecules TMS and tetrachlorocarbon ( $\text{CCl}_4$ ) in a variety of stretched gels with differing alignment strengths. The results are shown in Table 1: RDC values of up to 1 Hz were obtained as well as chemical shift differences of up to 100 ppb, clearly supporting previously measured data in liquid crystalline phases [70–73] and demonstrating that TMS can be partially aligned inside a stretched gel. Although it is unclear whether the chemical shift differences arise from  $\text{CCl}_4$ , TMS, or both,  $\Delta\sigma_{\text{mol}}^0$  of TMS appears not to be negligible, because expected RCSA values for small solute molecules are of



**Table 1**  
Evidence for Alignment of TMS in Stretched Gels.

Sample	$\Delta\nu_Q(\text{CDCl}_3)$ (Hz) <sup>a</sup>	$^1T_{\text{CH}}$ (Hz) <sup>b</sup>	$\sigma(^{13}\text{C}, \text{CCl}_4) - \sigma(^{13}\text{C}, \text{TMS})$ (ppm) <sup>c</sup>	$\Delta(\sigma(^{13}\text{C}, \text{CCl}_4) - \sigma(^{13}\text{C}, \text{TMS}))$ (ppb) <sup>d</sup>
PS/CDCl <sub>3</sub> <sup>e</sup> , low stretching	2.6 ± 1.0	118.17 ± 0.1	96.7722 ± 0.0032	7.5
PS/CDCl <sub>3</sub> <sup>e</sup> , high stretching	213.0 ± 10.0	117.71 ± 0.1	96.6629 ± 0.0032	−101.8
PU/CDCl <sub>3</sub> <sup>f</sup> , low stretching	0.0 ± 0.2	118.02 ± 0.1	96.7333 ± 0.0032	−31.4
PU/CDCl <sub>3</sub> <sup>f</sup> , intm. stretching	148.0 ± 5.0	118.11 ± 0.1	96.7080 ± 0.0032	−56.6
PU/CDCl <sub>3</sub> <sup>f</sup> , high stretching	450.0 ± 10.0	118.26 ± 0.1	96.6848 ± 0.0032	−79.8
CDCl <sub>3</sub> , low conc.	0.0	118.19 ± 0.1	96.7611 ± 0.0032	−3.5
CDCl <sub>3</sub> , high conc.	0.0	118.24 ± 0.1	96.7646 ± 0.0032	0.0
C <sub>6</sub> D <sub>6</sub> , high conc.	0.0	118.02 ± 0.1	96.9102 ± 0.0032	145.6

<sup>a</sup> Measured from <sup>2</sup>H 1D spectra.

<sup>b</sup>  $^1T_{\text{CH}} = ^1J_{\text{CH}} + ^1D_{\text{CH}}$ .

<sup>c</sup> Carbon chemical shift difference between CCl<sub>4</sub> and TMS measured on a Bruker Avance 250 spectrometer.

<sup>d</sup> Deviation of carbon chemical shift difference of CCl<sub>4</sub> and TMS with respect to the isotropic CDCl<sub>3</sub> sample.

<sup>e</sup> Poly(styrene) samples crosslinked with different amounts of divinylbenzene [43,48].

<sup>f</sup> Poly(urethane) samples of different diameter crosslinked by 120 kGy accelerated electrons.

similar order as the measured differences. Our next step therefore was to calibrate  $\Delta\sigma_{\text{mol}}^0$  of TMS in PDMS/CDCl<sub>3</sub> gels, which we later on wanted to use for applications.

### 3.3. Correction of chemical shift values as derived from theory

Since we wanted to measure  $\Delta\sigma_{\text{mol}}^0$  of the internal chemical shift standard, we were forced to use an external reference for standardization. In this case the chemical shift measurement of the desired internal reference relative to the external reference (indexed with an *e*) can be described by

$$\begin{aligned} \sigma_{\text{ext}}^{\text{iso},0} &= \sigma^{\text{iso},0} - \sigma^{\text{iso},e} \\ &= \sigma_{\text{mol}}^0 + \sigma_{\text{local}}^0 + \sigma_{\text{bulk}}^0 - \sigma_{\text{mol}}^e - \sigma_{\text{local}}^e - \sigma_{\text{bulk}}^e. \end{aligned} \quad (8)$$

Taking into account the vanishing  $\Delta\sigma_{\text{local}}^0$  and the fact that the external reference is not aligned, the corresponding measurement in an anisotropic sample will result in

$$\begin{aligned} \sigma_{\text{ext}}^{\text{aniso},0} &= \sigma^{\text{aniso},0} - \sigma^{\text{iso},e} \\ &= \sigma_{\text{ext}}^{\text{iso},0} + \Delta\sigma_{\text{bulk}}^0 + \Delta\sigma_{\text{mol}}^0. \end{aligned} \quad (9)$$

For  $\Delta\sigma_{\text{mol}}^0$  this implies that it can be measured as long as the bulk contribution to the chemical shift  $\Delta\sigma_{\text{bulk}}^0$  is known. Concerning the experiment this means that the overall shape and the susceptibility of the polymer should be identical in the isotropic and aligned samples.

For practically implementing the  $\Delta\sigma_{\text{mol}}^0$  measurement, we started with the chemical shift changes of  $\sigma_{\text{ext}}^{\text{iso},0}$  of TMS with respect to variation of the polymer content of corresponding linear, non-crosslinked PDMS/CDCl<sub>3</sub> as the isotropic matrix. For this we prepared several samples in 5 mm tubes with linear polymer contents (DMS-T61, 1000000 cSt., ABCR GmbH & Co KG) of 0–68% (w/v), which was verified by integration of <sup>1</sup>H spectra. We took special care that the filling height of the sample well exceeded the active height of the probehead coil in order to have comparable conditions for the anisotropic samples to be measured later on. The 5 mm tubes were then inserted into an 8 mm tube as shown in Fig. 3, with the outer volume of the sample construct being filled with 1% CHCl<sub>3</sub> in CDCl<sub>3</sub> for the external reference. Each sample was equilibrated for 15 min at 300 K in a Bruker Avance 500 MHz wide bore spectrometer equipped with an 8 mm liquid state TXI probehead with identical shim settings for all samples. We then measured a <sup>1</sup>H 1D spectrum, a <sup>2</sup>H 1D spectrum, and a <sup>1</sup>H,<sup>13</sup>C-CLIP-HSQC without locking the sample. For all gels the polymer content was measured by integration of <sup>1</sup>H 1D spectra with the integral of the external reference as the reference integral. The CLIP-HSQC spectra [74] with broadband optimized pulses [75–79] were recorded with 512 increments in the indirect dimension and a sweep width of only 150 Hz to ensure a digital resolu-

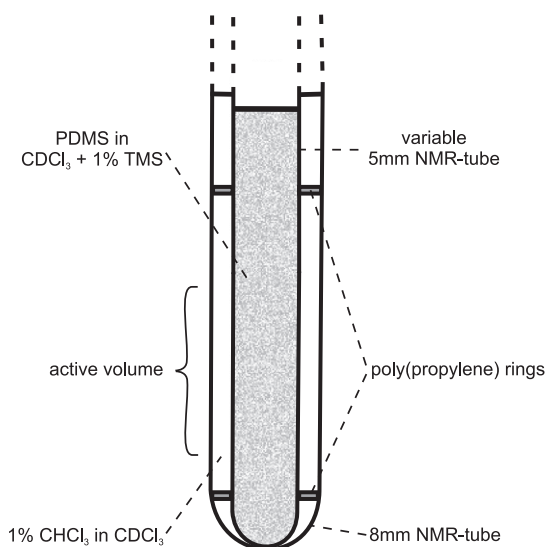


**Fig. 3.** Setup for potentially measuring the anisotropic chemical shift contribution to the internal reference TMS. For the measurement of different samples the inner 5 mm tube is exchanged.

tion below 0.3 Hz. The center frequency was set to 77.2 ppm, so that the chemical shift of CHCl<sub>3</sub> as the external reference was detected directly and the TMS signal was folded 31 times (which was proven with control HSQC experiments with larger sweep widths and lower resolution).

The difference of the <sup>13</sup>C chemical shifts of TMS and the external reference CHCl<sub>3</sub> are shown in Fig. 4 with filled circles. Clearly a linear dependence with the polymer content can be fitted to the result, corresponding to the expected chemical shift change to the varying bulk susceptibilities in the various samples.

In a second step, we then did identical measurements with the identical setup using 5 mm tubes with a number of swollen and stretched PDMS/CDCl<sub>3</sub> gels prepared as previously described [21] starting from the same starting material as the linear polymer (DMS-T61, 1000000 cSt., ABCR GmbH & Co KG). PDMS sticks of 2.4–4.0 mm diameters and crosslinked by irradiation doses between 100 kGy and 480 kGy of accelerated electrons were used. As for the isotropic samples, the polymer content was measured by integration of <sup>1</sup>H 1D spectra with the integral of the external reference as the reference integral. The corresponding chemical shift differences are also plotted in Fig. 4a, but with open symbols. Again the chemical shift difference follows the linear dependence of the non-crosslinked polymer, but an additional deviation is visible for the stretched gels, which should correspond to the desired  $\Delta\sigma_{\text{mol}}^0$  of TMS.

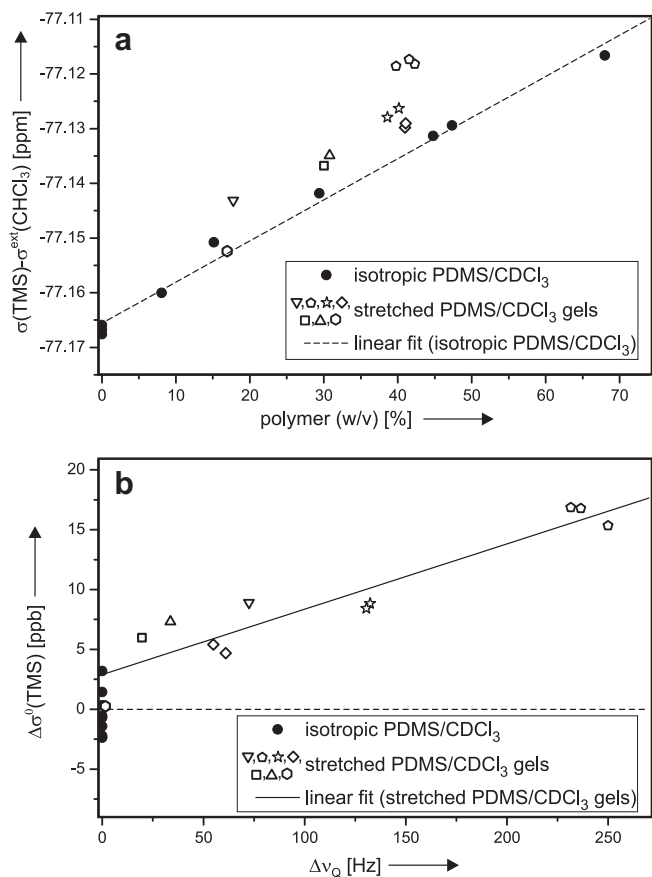


**Fig. 4.** (a) Chemical shift differences of TMS as internal reference relative to the external CHCl<sub>3</sub> using the setup shown in Fig. 3 vs. the concentration of PDMS as determined by integration of the corresponding signals of the <sup>1</sup>H 1D spectra. Values are shown for non-crosslinked PDMS (filled circles) as well as for stretched, crosslinked PDMS (open symbols). The concentration dependence of non-crosslinked PDMS can be described by a linear fit (dashed line). (b) After subtraction of the concentration dependence of non-crosslinked PDMS using the linear fit shown in (a), the residual chemical shift changes are plotted against the quadrupolar splitting  $\Delta\nu_Q$  of the corresponding CDCl<sub>3</sub> signals in the deuterium spectra. Again, a linear dependence can be derived (solid line and Eq. (10)).

In order to get a correction function for  $\Delta\sigma_{\text{mol}}^0$  for TMS in PDMS/CDCl<sub>3</sub> gels, we then plotted the differences  $\sigma_{\text{ext}}^{\text{aniso},0} - \sigma_{\text{ext}}^{\text{iso},0}$  by subtracting the corresponding values from the linear fit shown in Fig. 4a. The resulting plot with respect to the deuterium quadrupolar splitting  $\Delta\nu_Q$  as measured from <sup>2</sup>H 1D spectra is shown in Fig. 4b. With the assumption that the bulk susceptibility of crosslinked PDMS is identical to the bulk susceptibility of linear PDMS, the slope of the graph directly corresponds to  $\Delta\sigma_{\text{mol}}^0$ . With a linear fit of the results, we can derive the function

$$\Delta\sigma_{\text{mol}}^0(\Delta\nu_Q) = 0.055 \frac{\text{ppb}}{\text{Hz}} \cdot \Delta\nu_Q + 2.9 \text{ ppb} \quad (10)$$

with  $\Delta\nu_Q$  in Hz and  $\Delta\sigma_{\text{mol}}^0(\Delta\nu_Q)$  in parts per billion (ppb) for TMS in the polymer/solvent combination PDMS/CDCl<sub>3</sub>. With the easily measurable deuterium quadrupolar splitting and Eq. (10) we now can derive  $\Delta\sigma_{\text{mol}}^0$  of the internal reference TMS and therefore, according to Eq. (7), obtain the desired  $\Delta\sigma_{\text{mol}}^0$  of the solute molecule.

### 3.4. Empirical correction of chemical shift values

More empirical approaches for the correction of experimental chemical shift values against RCSA of the reference can be based

on the correlation of experimental data with back-calculated chemical shifts derived from theoretically obtained CSA-tensors.

As long as the alignment tensor for a molecular model can be estimated (either from RDC-measurements or e.g. cross-fitting of alignment [29]), expected RCSA values can be used for a linear fit

$$\Delta\sigma_{\text{mol}}(\text{calc}) = \Delta\sigma(\text{exp}) + c \quad (11)$$

of all experimental chemical shift changes upon alignment. The constant  $c$  then determines the deviation of experimental chemical shift values due to the partially aligned reference molecule. The resulting correction assumes that the alignment tensor used for the RCSA backcalculation is correct. For a rigid molecule the obtained RCSA values can then in principle be used to refine the alignment tensor and iterate the chemical shift correction  $c$  until both back-calculated and experimental RCSA values converge. For partially flexible molecules with potentially differing alignment tensors for different parts of the molecule, the RCSA backcalculation is of course more difficult and an iterative approach might even lead to wrong conclusions as more than one solution for the correction  $c$  might exist.

A second empirical approach, on the other hand, uses chemical shift values from a handful of carbons with the smallest predicted CSA tensors. Such carbons are typically methyl groups or other aliphatic groups. If experimental chemical shifts of carbon atoms with low CSA tensors are available, their average uncorrected RCSA can be assumed to correspond to the chemical shift change of the reference upon alignment. For an estimate, one can even use a single carbon atom as a start, bearing in mind that a small contribution due to the RCSA of the aliphatic group might still remain. The advantage of this approach is certainly that it can also be applied when no estimation of the alignment tensor is possible, which should be the common situation when a molecule with unknown configuration or conformation is studied and only a limited number of RDCs is available. The difficulty of the approach is the choice of the correct aliphatic atom(s) for the correction. The best choice for carbon atoms with the smallest chemical shift anisotropy are usually methyl groups. In the absence of methyl groups (as for example in the case of strychnine) it is convenient to look at a subset of carbon atoms with the lowest anisotropy of the calculated CSA-tensor for a given structural model. In unfavorable cases the method might not be applicable because of the absence of atoms with sufficiently small anisotropies. It should also be noted that the CSA-tensor depends strongly on the correct constitution and to some extent on the configuration and conformation of the structural model chosen.

### 4. Application to RCSA measurement: strychnine in PDMS/CDCl<sub>3</sub>

For demonstration of RCSA measurement with variable angle NMR we chose strychnine as a well-known test molecule for which residual dipolar couplings have been measured several times [3–5,43,74]. An aligned sample was prepared following the description shown in Fig. 1b using a PDMS stick of 3 mm diameter, irradiated with altogether 480 kGy of accelerated electrons, for swelling inside the 4 mm glass tube. The swelling was initiated by adding a solution of CDCl<sub>3</sub> containing approximately 5% TMS and 0.06 g/mL strychnine. After three weeks of equilibration, D<sub>2</sub>O and the sealing with a poly(ethylene) plug was added (see Fig. 1b). We then measured four experiments, a <sup>1</sup>H 1D spectrum, a <sup>2</sup>H 1D spectrum, a CLIP-HSQC with broadband pulses covering the whole chemical shift range of protons and carbons, and a <sup>1</sup>H-decoupled <sup>13</sup>C 1D spectrum, for each of the three selected angles  $\theta$ . While spectra for  $\theta = 54.7^\circ$  and  $\theta = 65^\circ$  were measured with a Bruker MAS probehead, the measurements at  $\theta = 0^\circ$  were performed in a TXI liquid state probehead with the sample put

inside a 5 mm NMR tube.  $^1\text{D}_{\text{CH}}$  RDCs for the sample were extracted from the differences in CLIP-HSQC spectra (see Fig. 5 and Table 2). Relatively strong alignment with corresponding large multiplet widths and strong coupling artifacts in some signals led to signal overlap (e.g. C15-H15a/b) and generally relatively large errors, but the corresponding alignment tensor could be determined using the program PALES with the -bestFit option for a conventional SVD fit in a straight forward way (see Table 3 for  $\Theta = 0^\circ$ ). We then measured all  $^{13}\text{C}$  chemical shifts relative to the internal reference TMS from the decoupled  $^{13}\text{C}$  1D spectra (see Fig. 6 and Table 4). With  $|\Delta\nu_Q| = 230 \pm 20$  Hz for  $\Theta = 0^\circ$  and  $|\Delta\nu_Q| = 55 \pm 15$  Hz for  $\Theta = 65^\circ$ , the corresponding correction in the PDMS/ $\text{CDCl}_3$  gel according to Eq. (10) is  $+15.5$  ppb and  $-5.9$  ppb, respectively. It should be noted that the spectral quality at the three angles differed significantly: while the high resolution probehead guaranteed narrow line-widths at  $\Theta = 0^\circ$ , broader lines are obtained with the solid state MAS probehead. With the particular probehead used in this study, the by far worst spectra with the lowest signal-to-noise-ratio were obtained at  $\Theta = 65^\circ$  with the broadest lines and a nonsymmetric lineshape (see Fig. 6). For the proof of principle we therefore decided to continue with the RCSA values from the difference between the most reliable chemical shifts at  $\Theta = 0^\circ$  and  $\Theta = 54.7^\circ$ , which are also the most widely accessible angles with common solid and liquid state NMR equipment.

Carbon CSA-tensors for a comparison of experimental and back-calculated RCSA values were then derived by an ab initio approach. The strychnine CSA-tensors and scalar coupling constants were estimated using GIAO B3LYP/cc-pVDZ method on B3LYP/cc-pVDZ

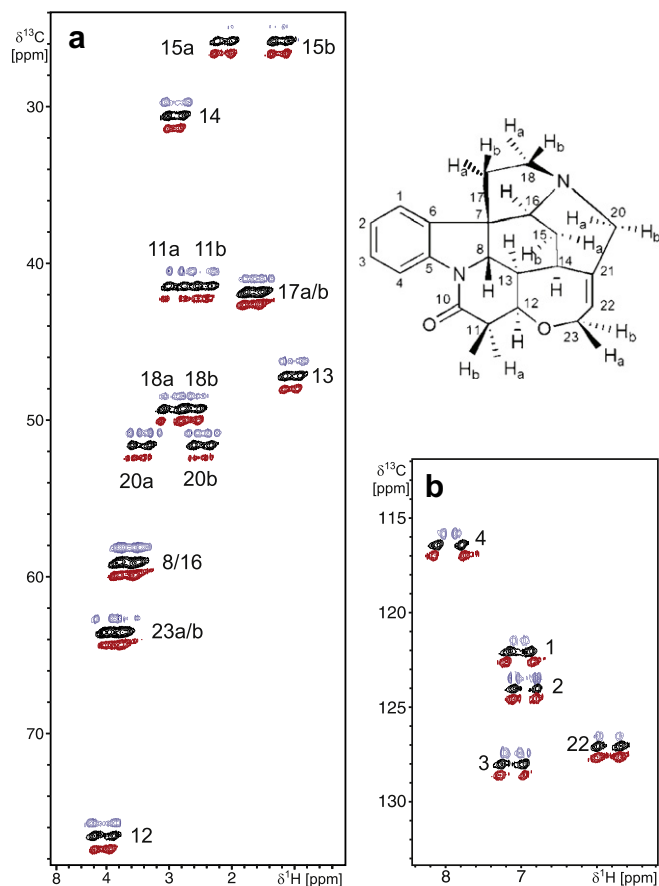


**Fig. 5.** CLIP-HSQC spectra [74] measured on strychnine diffused into a stretched PDMS/ $\text{CDCl}_3$  gel as described in the main text at  $\Theta = 54.7^\circ$  (black),  $\Theta = 0^\circ$  (blue, dark gray), and  $\Theta = 65^\circ$  (red, light gray). The individual spectra have been shifted in the  $^{13}\text{C}$  dimension for clarity. (For interpretation of the references to colour in this figure legend, the reader is referred to the web version of this article.)

**Table 2**

One-bond scalar and residual dipolar couplings measured for strychnine in PDMS/ $\text{CDCl}_3$ .

Bond	$^1\text{T}_{\text{CH}}$ , $\Theta = 54.7^\circ$ (Hz) <sup>a</sup>	$^1\text{D}_{\text{CH}}$ , $\Theta = 0^\circ$ (Hz) <sup>b</sup>	$^1\text{D}_{\text{CH}}$ , $\Theta = 65^\circ$ (Hz) <sup>c</sup>
C1-H1	150.2 ± 5.0	-72.2 ± 9.4	35.3 ± 5.4
C2-H2	161.7 ± 2.0	n. a. <sup>d</sup>	-1.5 ± 3.6
C3-H3	155.8 ± 10.0	n. a. <sup>d</sup>	14.4 ± 10.4
C4-H4	166.0 ± 5.0	-86.0 ± 7.1	36.2 ± 5.4
C11-H11a	129.1 ± 5.0	-34.3 ± 5.4	15.3 ± 7.1
C11-H11b	120.0 ± 5.0	56.7 ± 6.4	-35.8 ± 7.1
C12-H12	155.8 ± 10.0	33.0 ± 5.8	-28.7 ± 10.2
C13-H13	117.7 ± 5.0	22.3 ± 20.6	-12.7 ± 5.4
C14-H14	129.7 ± 5.0	50.1 ± 5.4	-26.7 ± 5.6
C15-H15a	118.3 ± 5.0	n. a. <sup>e</sup>	15.8 ± 5.1
C15-H15b	117.7 ± 5.0	n. a. <sup>e</sup>	3.5 ± 5.8
C20-H20a	138.2 ± 3.0	20.8 ± 5.8	-14.2 ± 7.6
C20-H20b	136.5 ± 3.0	16.9 ± 5.8	-9.5 ± 7.6
C22-H22	158.2 ± 3.0	-14.9 ± 10.2	-1.5 ± 3.4

<sup>a</sup> Measured splitting close to the magic angle, should be very close to  $^1\text{J}_{\text{CH}}$ .

<sup>b</sup> Dipolar splitting contribution measured as the difference  $^1\text{T}_{\text{CH}}(\Theta = 0^\circ) - ^1\text{T}_{\text{CH}}(\Theta = 54.7^\circ)$ .

<sup>c</sup> Dipolar splitting contribution measured as the difference  $^1\text{T}_{\text{CH}}(\Theta = 65^\circ) - ^1\text{T}_{\text{CH}}(\Theta = 54.7^\circ)$ .

<sup>d</sup> No reliable measurement possible due to second order artifacts.

<sup>e</sup> Too low signal intensity.

**Table 3**

Alignment Tensor Parameters Derived from RDCs Measured at  $\Theta = 0^\circ$ .<sup>a</sup>

Eigen values ( $A_{xx}, A_{yy}, A_{zz}$ )	4.1233e-04	1.4425e-03	-1.8548e-03
Eigen vectors, x	8.5354e-01	-5.1739e-01	6.1508e-02
Eigen vectors, y	-6.1282e-02	1.7543e-02	9.9797e-01
Eigen vectors, z	5.1741e-01	8.5557e-01	1.6733e-02
$D_a, D_r$	-9.274096e-04	-3.433886e-04	
RMS, R, Q <sup>b</sup>	6.969 Hz	0.989	0.148

<sup>a</sup> All data taken from the output of the corresponding PALES SVD fit.

<sup>b</sup> All parameters as described in [54]. RMS: root mean square deviation; R: correlation factor R; Q: Cornilescu Q-factor.

optimized geometry. For the calculation of scalar couplings, the basis set was decontracted and augmented with tight functions around the nucleus. All calculations were carried out using Gaussian03. The individual principal components of the individual carbon CSA-tensors of strychnine are summarized in Table 5.

With the ab initio  $^{13}\text{C}$ -CSA-tensors  $\sigma_{\alpha\beta}$  and the RDC-derived alignment tensor  $A_{\alpha\beta}$  in hand, the corresponding expected RCSA  $\Delta\sigma_{\text{mol}}$  values were back-calculated according to

$$\Delta\sigma_{\text{mol}} = \sum_{\alpha,\beta=x,y,z} \sigma_{\alpha\beta} A_{\alpha\beta}. \quad (12)$$

Back-calculated RCSA values were then compared to experimental values using the different approaches for determination of  $\Delta\sigma_{\text{mol}}^0$  (Fig. 7). The theoretical correction of the reference was determined using Eq. (10) to be 15.5 ppb. Apparently, there is a good linear correlation, but a constant offset of  $\approx 50$  ppb is noticeable in the linear fit for the theoretically corrected RCSA values (Fig. 7a). On the other hand, the empirical approaches for determination of  $\Delta\sigma_{\text{mol}}^0$  lead to linear correlations with offsets smaller than the average experimental error (see Fig. 7b and Fig. 7c). For the first empirical approach a least square fit according to Eq. (11) over all carbon atoms was performed and  $c = -35.5$  ppb was obtained as the correction for  $\Delta\sigma_{\text{mol}}^0$  (Fig. 7b). For the second approach the three aliphatic carbons C13, C14, and C15 as the three nuclei with the smallest theoretically determined anisotropy of the CSA tensor, defined as  $\sigma_{33} - (\frac{\sigma_{11} + \sigma_{22}}{2})$  (see also Table 5), were chosen and their averaged uncorrected experimental RCSA value ( $-33.9$  ppb) used as the correction (Fig. 7c).

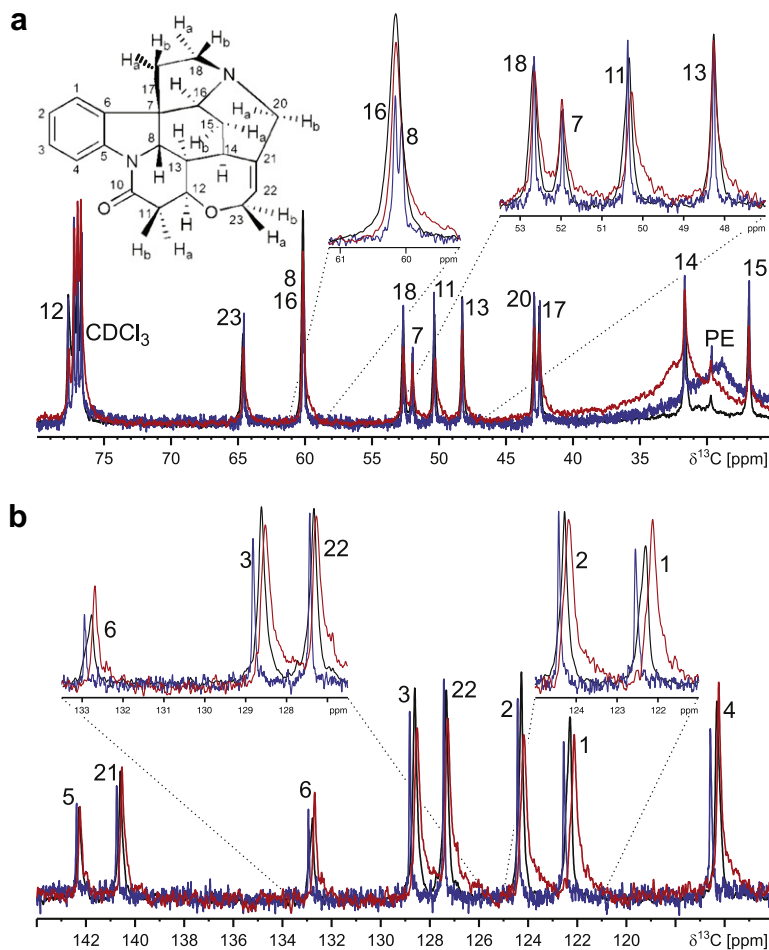


**Fig. 6.** Aliphatic (a) and aromatic (b) regions of  $^{13}\text{C}$  1D spectra measured on strychnine diffused into a stretched PDMS/ $\text{CDCl}_3$  gel as described in the main text at  $\Theta = 54.7^\circ$  (black),  $\Theta = 0^\circ$  (blue, dark gray), and  $\Theta = 65^\circ$  (red, light gray). NMR signals originating from the poly(ethylene) plug are marked with PE. Spectra are referenced to C13/C14/C15 as the carbons with smallest RCSA-tensors (see also Fig. 7c and main text). (For interpretation of the references to colour in this figure legend, the reader is referred to the web version of this article.)

**Table 4**  
Chemical shifts and RCSA values measured for strychnine in PDMS/ $\text{CDCl}_3$  relative to the internal reference TMS without correction.

	$\sigma, \Theta = 54.7^\circ$ (ppm)	$\Delta\sigma, \Theta = 0^\circ$ (ppb) <sup>a</sup>	$\Delta\sigma, \Theta = 65^\circ$ (ppb)
C1	122.24 ± 0.01	310 ± 15	-149 ± 16
C2	124.22 ± 0.01	211 ± 12	-81 ± 13
C3	128.56 ± 0.01	267 ± 12	-73 ± 13
C4	116.27 ± 0.01	321 ± 13	-60 ± 14
C5	142.21 ± 0.01	182 ± 11	-11 ± 14
C6	132.72 ± 0.01	224 ± 15	-62 ± 16
C7	51.98 ± 0.01	24 ± 11	15 ± 14
C8	60.14 ± 0.02	-58 ± 25 <sup>b</sup>	n. a. <sup>c</sup>
C11	42.51 ± 0.01	8 ± 11	15 ± 13
C12	77.65 ± 0.01	65 ± 14	-16 ± 16
C13	48.26 ± 0.01	41 ± 11	19 ± 13
C14	31.66 ± 0.01	57 ± 12	18 ± 14
C15	26.89 ± 0.01	3 ± 11	18 ± 13
C16	60.14 ± 0.02	38 ± 25 <sup>b</sup>	n. a. <sup>c</sup>
C17	42.89 ± 0.01	50 ± 11	-3 ± 14
C18	50.34 ± 0.01	71 ± 12	-37 ± 14
C20	52.67 ± 0.01	29 ± 12	-12 ± 14
C21	140.53 ± 0.01	220 ± 11	-49 ± 13
C22	127.28 ± 0.01	162 ± 11	-36 ± 13
C23	64.61 ± 0.01	-15 ± 12	-12 ± 14
$\text{CDCl}_3$	76.95 ± 0.01	26 ± 11	19 ± 13

<sup>a</sup> For the correction of chemical shift values see Fig. 7 and main text.

<sup>b</sup> Assignment of C8/C16 based on back-calculated RCSA values (see Figs. 7 and 8).

<sup>c</sup> Not measurable due to overlap.

Although we chose strychnine as a well-studied test molecule, for which generally no surprising results are expected, we had two interesting observations during the extraction of RCSA values which highlight the potential usefulness of such data for the veri-

**Table 5**  
Calculated carbon CSA tensor parameters for strychnine in ppm.

Atom	$\sigma_{11}$	$\sigma_{22}$	$\sigma_{33}$	$\sigma_{iso}$	$\sigma_{33} - (\frac{\sigma_{11} + \sigma_{22}}{2})$
C1	-24.2184	58.0796	181.6335	71.8315	164.7029
C2	-27.4997	60.0028	178.1613	70.2215	161.9098
C3	-34.7749	50.3175	178.4750	64.6725	170.7037
C4	-3.8292	52.1655	179.3619	75.8994	155.1937
C5	-37.6607	54.5057	130.3236	49.0562	121.9011
C6	-8.0151	35.7231	153.3156	60.3412	139.4616
C7	122.9718	127.5874	153.3397	134.6329	28.0601
C8	103.7440	128.5806	154.3884	128.9043	38.2261
C10	-55.0797	41.5919	97.9394	28.1505	104.6833
C11	124.9007	143.2204	173.9766	147.3659	39.9161
C12	92.5960	96.2883	145.2023	111.3622	50.7601
C13	124.7802	141.1792	153.3583	139.7726	20.3786
C14	144.8587	157.0315	162.9913	154.9605	12.0463
C15	148.0326	165.3956	171.2385	161.5556	14.5243
C16	104.2863	128.5723	152.8405	128.5663	36.4112
C17	123.8848	139.4994	174.5121	145.9654	42.8200
C18	106.2374	139.4275	177.9555	141.2068	55.1230
C20	126.9121	132.0522	156.5421	138.5021	27.0599
C21	-50.9251	41.9848	154.2627	48.4408	158.7328
C22	-35.6423	82.4552	148.0998	64.9709	124.6933
C23	98.2741	109.1328	171.9649	126.4573	68.2615



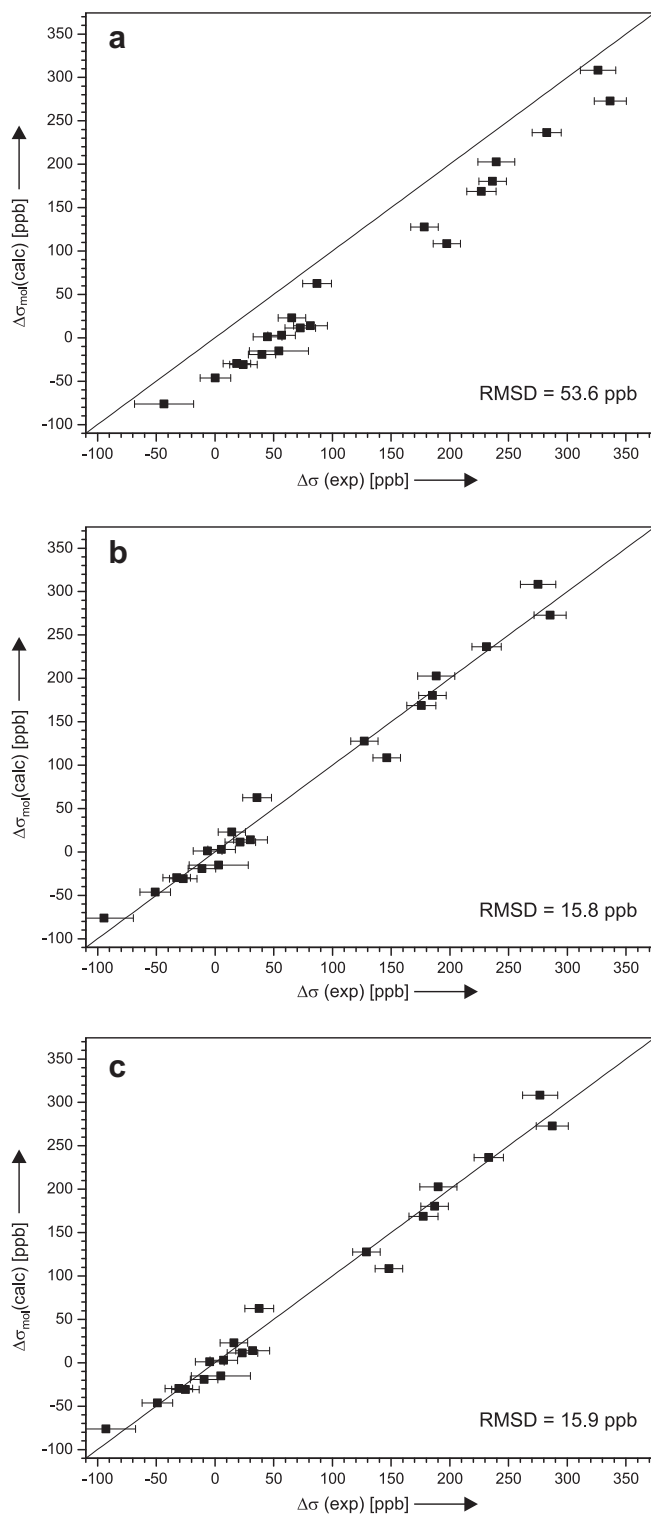


**Fig. 7.** Back-calculated  $\Delta\sigma_{\text{mol}}(\text{calc})$  vs. experimental  $\Delta\sigma(\text{exp})$  residual chemical shift anisotropies for strychnine in PDMS/ $\text{CDCl}_3$  with various corrections to the reference. (a) Corrections as derived from Eq. (10), (b) correction with a least square fit over all uncorrected RCSA values, (c) correction by the average uncorrected RCSA value for C13, C14, and C15 as the three nuclei with the smallest theoretically determined CSA tensor.

fication of structural models and the assignment of resonances. The first observation was due to an accidental mis-assignment: by chance we missed a line and wrongly read off chemical shift values from a list and thereby switched the assignment of the carbons C1 and C2 with RCSA values of 277 ppb and 178 ppb. We did not

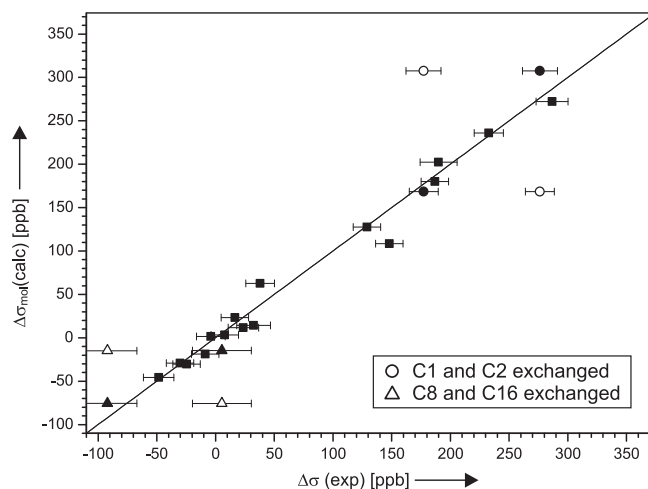


**Fig. 8.** Back-calculated  $\Delta\sigma_{\text{mol}}(\text{calc})$  vs. experimental  $\Delta\sigma(\text{exp})$  residual chemical shift anisotropies for strychnine in PDMS/ $\text{CDCl}_3$  with the correction to the reference as in Fig. 7c (filled symbols). As described in more detail in the main text, the accidental misassignment of C1 and C2 (open and filled circles) could be identified by the plot shown. In the same way carbons C8 and C16, which overlap in the isotropic spectrum, can unambiguously be assigned (open and filled triangles).

notice until we plotted back-calculated and experimental RCSA values (Fig. 8). Our initial disappointment of the bad match of results soon turned into a pleasant surprise when we looked again into the original data and found the erroneous assignment.

Our second positive experience concerns the assignment of overlapping signals. By chance, resonances of carbons C8 and C16 strongly overlap in the  $^{13}\text{C}$  1D spectrum at the magic angle and an unambiguous assignment in the isotropic spectrum is not possible. In the spectrum at  $\theta = 0^\circ$ , however, the two signals separate and defined RCSA values of 5.5 ppb and  $-93$  ppb (after correction according to Fig. 7c) can be determined. While an assignment of the two signals is not possible *a priori* from the acquired spectra, the analysis of back-calculated RCSA values results in an unambiguous identification of signals (Fig. 8).

## 5. Discussion

In this article we describe the scaling of partial alignment with a single stretched gel sample by varying the angle of the director with respect to the static magnetic field, which we call variable angle NMR (VA-NMR). The scaling of alignment and therefore the measurement of anisotropic NMR parameters like RDCs, RQCs, and RCSAs in a single sample has several advantages with respect to the number of samples to be prepared, material needed, time saved, and the accuracy and comparability of measured data. Variable angle NMR spectroscopy with stretched gels as alignment media is a very effective technique which can be applied easily as long as a VASS or MAS probehead is available. The method is strongly related to variable angle sample spinning of liquid crystalline phases, but it is generally easier to apply as no spinning rate has to be adjusted and samples can be prepared in a more cost-effective way in NMR glass tubes. Moreover, as mentioned before, VASS-NMR is usually limited to tilt ranges between  $0^\circ \leq \theta < 54.7^\circ$  or  $54.7^\circ < \theta \leq 90^\circ$ , respectively, depending on the sign of the magnetic susceptibility anisotropy of the liquid crystal. The corresponding complementary angular ranges are only accessible by using a different liquid crystalline phase or by adding e.g. lanthanide ions to phospholipid bicelles, thereby changing the composition of the overall sample. In contrast, VA-NMR with stretched gels covers the full range of  $0^\circ \leq \theta \leq 90^\circ$  in a single

unmodified sample as the director of alignment is fully determined by the mechanical stretching of the gel.

Scaling of alignment using a silicone-rubber-based stretching apparatus [58–60] is another technique with the advantage of being applicable with no change in the environment of the solute molecule and conventional liquid state NMR equipment. The approach has recently been extended to nonpolar solvents by the use of perfluorinated elastomer tubings [61] and might be used in an equivalent way for measuring RCSA values. The main limitations of this approach is again the limited range of scaling factors in covalently crosslinked gels corresponding to  $0^\circ \leq \Theta \leq 54.7^\circ$  in the VA-NMR approach.

A third way of scaling alignment, the defined compression of gels with a glass rod in a conventional NMR tube [39,62], requires even less specialized equipment. However, upon compression, in this case, the concentration of the crosslinked polymer increases as the solvent is pressed out of the gel. As a consequence one loses the advantage of a constant environment for the solute molecule and measurement of very sensitive parameters like RCSA will become less reliable.

It must be mentioned that many reported RCSA measurements are performed in two different samples or in a single sample below and above the liquid crystalline phase transition temperature. It has been shown previously that the alignment medium works as a kind of co-solvent with sometimes very strong effects on the chemical shift values (see e.g. [48,49] for an impressive example). Although maybe weaker, the same effect must be expected for an isotropic to liquid crystalline phase transition. The phase transition is usually of first order, meaning that an abrupt jump of all physical properties will occur at the transition temperature. Therefore the extrapolation of temperature curves from the isotropic to the liquid crystalline phase and vice versa are of no use. Some clear examples for this have been summarized e.g. in [65]. These problems are of course overcome by measuring the anisotropic parameters within a single sample at identical conditions like concentration, temperature, etc.

The measurement of chemical shift values is usually done by measuring the difference to an internal reference like TMS. For an accurate determination of RCSAs it is therefore necessary to ensure that this reference is not affected by alignment. However, as has been previously shown for a number of molecules with even tetrahedral symmetry [65], RCSA contributions to the chemical shift of the reference molecule will occur due to the vibration-reorientation interaction and thus cannot be neglected. It must be expected that this effect will be even stronger for reference molecules with lower symmetry than tetrahedral TMS, so one has to take special care with water samples with TSP or DSS as the reference, for example.

We put here quite some effort in a theoretical derivation and quantitative measurement of the corresponding chemical shift correction to the reference TMS. Unfortunately, the measured correction function for TMS did not lead to a good correlation of experimental and back-calculated RCSA values. We do not yet fully understand this failure of the derived RCSA correction, but can only speculate on the potential reasons. From the experimental point of view, the derivation of the chemical shift correction was performed with linear polymer chains and gel samples crosslinked by irradiation. We therefore cannot fully exclude an effect of the irradiation dose on the susceptibility of the gel sample, in which case an increasing irradiation contribution to the measured chemical shift values with increasing alignment strength would be expected, with a correspondingly wrong slope of the linear fit shown in Fig. 4b and therefore a wrong correction function. On the other hand, the correction function was determined in a pure PDMS/chloroform sample while the full  $^{13}\text{C}$ -RCSA measurements were performed in the presence of approximately 10 mM strychnine. Weak interactions

between the solute and PDMS,  $\text{CDCl}_3$ , or TMS might be sufficient to cause different alignment properties for the reference. In this case, the RCSA contribution would depend on the particular solute molecule and the derivation of a general correction function would not make sense. Finally, the assumptions that  $\Delta\sigma_{\text{local}}^o$  and  $\Delta\sigma_{\text{local}}$  can be fully neglected might not be justified.

The two other, more empirical approaches for getting an estimate for the correction of the reference signal apparently both work well. As long as a given alignment tensor shall be verified by RCSA values, it is certainly best to use all RCSA information available for fitting  $\Delta\sigma_{\text{mol}}^o$  (Fig. 7b). However, if RCSA data are used for the derivation of an alignment tensor or any other model of alignment, the second approach based on the calibration to the average RCSA of a small number of signals with expected low CSA tensor is appropriate (Fig. 7c). The correction can of course also be done iteratively, starting with an initial estimate from the second empirical approach and using the then derived model for an improved correction with the first empirical approach.

It should be noted that both empirical approaches can also be used if no internal chemical shift reference substance is added to the sample. In this case one of the signals of the solute molecule itself can be used for reference and the RCSA correction can simply be applied relative to the RCSA value of the particular chosen signal.

Concerning the accuracy of chemical shift measurements it must be stated that it is quite high, especially for carbon chemical shifts measured at natural abundance where all signals can be reduced to singlets by heteronuclear decoupling. The achievable line-width of MAS probeheads is certainly lower than corresponding high resolution probeheads, but as long as signal-to-noise is sufficient, chemical shift values of singlets can be determined very straightforwardly. If more complex signal patterns are present, either due to more complex multiplets, strong coupling artifacts, or chemical/conformational exchange, corresponding errors will increase accordingly. The errors given in this article are the maximum error estimates which we obtained by the procedure originally described in [29] for the measurement of RDCs. Such maximum error estimates are at least three times the statistical variance and in an SVD fit of a structural model all back-calculated RCSA values should lie within the error boundaries. Other methods, as for example automated peak picking based on volume integration [80], might lead to RCSA values with even tighter error boundaries.

For the quality of fitting RCSA data, however, not only the experimental data, but even more critically also the predicted CSA-tensors have to be highly reliable. It is out of the scope of this article to deal with the many aspects of chemical shift prediction, but its potentially large error certainly remains as a difficult to quantify source of uncertainty. Nevertheless, RCSA in combination with one of the various scaling approaches should be routinely measurable and highly useful as an independent source of validation of a given structural model or even as input for structure determination or refinement, respectively.

Finally, it should be mentioned that VA-NMR is not limited to the measurement of RCSA, but can also be used effectively for measuring other anisotropic NMR parameters like residual dipolar and quadrupolar couplings. The scaling of alignment allows easily the adjustment to obtain maximum spectral quality for the coupling measurements. It can also be used to scale for example long-range RDCs, which are usually too small to discriminate between different structures (see e.g. [6]) when they are measured at the same alignment strength as one-bond RDCs. With VA-NMR the alignment strength can be tuned to accommodate the ideal range of values for each anisotropic parameter, including a sign-reversal of the interaction when crossing the magic angle.

## 6. Conclusion

In summary, we introduced variable angle NMR spectroscopy (VA-NMR) as a tool to scale the alignment strength in mechanically stretched gels. The method generally allows scaling over the full range of  $\frac{3}{2} \cos^2 \Theta - \frac{1}{2}$  for the angle  $\Theta$  between the director of gel stretching and the static magnetic field. As no sample spinning is required with this method, sample preparation can be accomplished in simple glass tubes without the need of expensive rotors.

The method allows the measurement of anisotropic NMR parameters in a single sample. In particular for the measurement of residual chemical shift anisotropy (RCSA) this is of great advantage as chemical shift changes due to the addition of the alignment medium [48,49] can be avoided. The reliability and applicability of RCSA values measured in this way are demonstrated for strychnine aligned in a stretched PDMS/CDCl<sub>3</sub> gel. In this context, particular care has been taken in the determination of RCSA effects on the internal reference TMS.

## Acknowledgments

The authors gratefully acknowledge the DFG-Center for Functional Nanostructures at the Karlsruhe Institute of Technology for financing part of the NMR infrastructure (E1.2). B.L. also thanks the Center for Integrated Protein Science Munich, the Fonds der Chemischen Industrie and the DFG for financial support (Heisenberg program LU 835/2,3,4,7). C.M.T. thanks the DFG for financial support (Emmy Noether program TH 1115/3-1) and M. Reggelin for his support.

## References

- [1] C.M. Thiele, Use of RDCs in rigid organic compounds and some practical considerations concerning alignment media, *Conc. Magn. Reson. A* 30 (2007) 65–80.
- [2] C.M. Thiele, Residual dipolar couplings (RDCs) in organic structure determination, *Eur. J. Org. Chem.* 34 (2008) 5673–5685.
- [3] G. Kummerlöwe, B. Luy, Residual dipolar couplings as a tool in determining the structure of organic molecules, *Trends Anal. Chem.* 28 (2009) 483–493.
- [4] G. Kummerlöwe, B. Luy, Residual dipolar couplings for the configurational and conformational analysis of organic molecules, *Annu. Rep. NMR Spectrosc.* 68 (2009) 193–232.
- [5] C.M. Thiele, S. Berger, Probing the diastereotopicity of methylene protons in strychnine using residual dipolar couplings, *Org. Lett.* 5 (2003) 705–708.
- [6] L. Verdier, P. Sakhaii, M. Zweckstetter, C. Griesinger, Measurement of long range H, C couplings in natural products in orienting media: a tool for structure elucidation of natural products, *J. Magn. Reson.* 163 (2003) 353–359.
- [7] E. Sackmann, S. Meiboom, L.C. Snyder, Nuclear magnetic resonance spectra of enantiomers in optically active liquid crystals, *J. Am. Chem. Soc.* 90 (1968) 2183–2184.
- [8] K. Czarniecka, E.T. Samulski, Polypeptide liquid-crystals – a deuterium NMR study, *Mol. Cryst. Liq. Cryst.* 63 (1981) 205–214.
- [9] E. Lafontaine, J.P. Bayle, J. Courtieu, High-resolution NMR in cholesteric medium – visualization of enantiomers, *J. Am. Chem. Soc.* 111 (1989) 8294–8296.
- [10] M. Sarfati, P. Lesot, D. Merlet, J. Courtieu, Theoretical and experimental aspects of enantiomeric differentiation using natural abundance multinuclear NMR spectroscopy in chiral polypeptide liquid crystals, *Chem. Commun.* (2000) 2069–2081.
- [11] K. Kobzar, H. Kessler, B. Luy, Stretched gelatin gels as chiral alignment media for the discrimination of enantiomers by NMR spectroscopy, *Angew. Chem., Int. Ed.* 44 (2005) 3145–3147; Corrigendum: *Angew. Chem., Int. Ed.* (2005) 3509.
- [12] U. Eliav, G. Navon, Collagen fibers as a chiral agent: a demonstration of stereochemistry effects, *J. Am. Chem. Soc.* 128 (2006) 15056–15057.
- [13] C. Naumann, P.W. Kuchel, NMR (pro)chiral discrimination using polysaccharide gels, *Chem. Eur. J.* 15 (2009) 12189–12191.
- [14] C. Naumann, W.A. Bubb, B.E. Chapman, P.W. Kuchel, Tunable-alignment chiral system based on gelatin for NMR spectroscopy, *J. Am. Chem. Soc.* 129 (2007) 5340–5341.
- [15] G. Kummerlöwe, M. Udaya Kiran, B. Luy, Covalently crosslinked gelatin allows the chiral distinction at elevated temperatures and in DMSO, *Chem. Eur. J.* 15 (2009) 12192–12195.
- [16] J.L. Yan, A.D. Kline, H.P. Mo, M.J. Shapiro, E.R. Zartler, The absolute sign of J coupling constants determined using the order matrix calculation, *Magn. Reson. Chem.* 42 (2004) 962–967.
- [17] J. Furrer, M. John, H. Kessler, B. Luy, J-Spectroscopy in the presence of residual dipolar couplings: determination of one-bond coupling constants and scalable resolution, *J. Biomol. NMR* 37 (2007) 231–243.
- [18] J.L. Yan, A.D. Kline, H.P. Mo, M.J. Shapiro, E.R. Zartler, A novel method for the determination of stereochemistry in six-membered chairlike rings using residual dipolar couplings, *J. Org. Chem.* 68 (2003) 1786–1795.
- [19] C. Aroulanda, V. Boucard, F. Guibe, J. Courtieu, D. Merlet, Weakly oriented liquid-crystal NMR solvents as a general tool to determine relative configurations, *Chem. Eur. J.* 9 (2003) 4536–4539.
- [20] J.L. Yan, F. Delaglio, A. Kaerner, A.D. Kline, H.P. Mo, M.J. Shapiro, T.A. Smitka, G.A. Stephenson, E.R. Zartler, Complete relative stereochemistry of multiple stereocenters using only residual dipolar couplings, *J. Am. Chem. Soc.* 126 (2004) 5008–5017.
- [21] J.C. Freudenberger, P. Spittler, R. Bauer, H. Kessler, B. Luy, Stretched polydimethylsiloxane gels as NMR-alignment media for apolar and weakly polar organic solvents: ideal tool for measuring RDCs at low molecular concentrations, *J. Am. Chem. Soc.* 126 (2004) 14690–14691.
- [22] C.M. Thiele, A. Marx, R. Berger, J. Fischer, M. Biel, A. Giannis, Determination of the relative configuration of a five-membered lactone from residual dipolar couplings, *Angew. Chem., Int. Ed.* 45 (2006) 4455–4460.
- [23] A. Schuetz, J. Junker, A. Leonov, O.F. Lange, T.F. Molinski, C. Griesinger, Stereochemistry of Sagittamide A from residual dipolar coupling enhanced NMR, *J. Am. Chem. Soc.* 129 (2007) 15114–15115.
- [24] A. Schuetz, T. Murakami, N. Takada, J. Junker, M. Hashimoto, C. Griesinger, RDC-enhanced NMR spectroscopy in structure elucidation of sucro-neolambertellin, *Angew. Chem., Int. Ed.* 47 (2008) 2032–2034.
- [25] C. Farés, J. Hassfeld, D. Menche, T. Carlomagno, Simultaneous determination of the conformation and relative configuration of Archazolidine A by using nuclear Overhauser effects, J couplings, and residual dipolar couplings, *Angew. Chem., Int. Ed.* 47 (2008) 3722–3726.
- [26] G. Kummerlöwe, S. Knör, A.O. Frank, T. Paululat, H. Kessler, B. Luy, Deuterated polymer gels for measuring anisotropic NMR parameters with strongly reduced artefacts, *Chem. Commun.* (2008) 5722–5724.
- [27] D. Intelmann, G. Kummerlöwe, G. Haseleu, N. Desmer, K. Schulze, R. Fröhlich, O. Frank, B. Luy, T. Hofmann, Structures of storage-induced transformation products of the beer's bitter principle, revealed by sophisticated NMR spectroscopy and LC/MS techniques, *Chem. Eur. J.* 15 (2009) 13047–13058.
- [28] J.D. Swarbrick, T.D. Ashton, NMR studies on dextromethorphan in both isotropic and anisotropic states, *Chirality* 22 (2010) 42–49.
- [29] G. Kummerlöwe, S. Schmitt, B. Luy, Cross-fitting of residual dipolar couplings, *The Open Spectrosc. J.* 4 (2010) 16–27.
- [30] M. Martín-Pastor, C.A. Bush, The use of NMR residual dipolar couplings in aqueous dilute liquid crystalline medium for conformational studies of complex oligosaccharides, *Carbohydr. Res.* 323 (2000) 147–155.
- [31] J. Adeyeye, H.F. Azurmendi, C.J.M. Stroop, S. Sozhamannan, A.L. Williams, A.M. Adetumbi, J.A. Johnson, C.A. Bush, Conformation of the hexasaccharide repeating subunit from the *Vibrio cholerae* O139 capsular polysaccharide, *Biochemistry* 42 (2003) 3979–3988.
- [32] J. Cramer, C. Neubauer, M. Coles, H. Kessler, B. Luy, Structure refinement of Cyclosporin A in chloroform by using RDCs measured in a stretched PDMS-gel, *ChemBioChem* 6 (2005) 1672–1678.
- [33] U.M. Reinscheid, J. Farjon, M. Radzom, P. Haberz, A. Zeeck, M. Blackledge, C. Griesinger, Effect of the solvent on the conformation of a depsiptide: NMR-derived solution structure of hormaomycin in DMSO from residual dipolar couplings in a novel DMSO-compatible alignment medium, *ChemBioChem* 7 (2006) 287–296.
- [34] N. Cramer, S. Helbig, A. Baro, S. Laschat, R. Diestel, F. Sasse, D. Mathieu, C. Richter, G. Kummerlöwe, B. Luy, H. Schwalbe, Synthesis and biological properties of cylindramide derivatives: evidence for calcium-dependent cytotoxicity of tetramic acid lactams, *ChemBioChem* 9 (2008) 2474–2486.
- [35] M. Udaya Kiran, A. Sudhakar, J. Klages, G. Kummerlöwe, B. Luy, B. Jagadeesh, RDC enhanced NMR spectroscopy in organic solvent media: the importance for the experimental determination of periodic hydrogen bonded secondary structures, *J. Am. Chem. Soc.* 131 (2009) 15590–15591.
- [36] B. Böttcher, V. Schmidts, J.A. Raskatov, C.M. Thiele, Determination of the conformation of the key intermediate in an enantioselective palladium-catalyzed allylic substitution from residual dipolar couplings, *Angew. Chem., Int. Ed.* 49 (2010) 205–209.
- [37] C. Aroulanda, M. Sarfati, J. Courtieu, P. Lesot, Investigation of the enantioselectivity of three polypeptide liquid-crystalline solvents using NMR spectroscopy, *Enantiomer* 6 (2001) 281–287.
- [38] R.Y. Dong, Nuclear Magnetic Resonance Spectroscopy on Liquid Crystals, World Scientific, Publishing, Singapore, 2010.
- [39] R. Tycko, F.J. Blanco, Y. Ishii, Alignment of biopolymers in strained gels: a new way to create detectable dipole–dipole couplings in high-resolution biomolecular NMR, *J. Am. Chem. Soc.* 122 (2000) 9340–9341.
- [40] H.J. Sass, G. Musco, S.J. Stahl, P.T. Wingfield, S. Grzesiek, Solution NMR of proteins within polyacrylamide gels: diffusional properties and residual alignment by mechanical stress or embedding of oriented purple membranes, *J. Biomol. NMR* 18 (2000) 303–309.
- [41] S. Meier, D. Haussinger, S. Grzesiek, Charged acrylamide copolymer gels as media for weak alignment, *J. Biomol. NMR* 24 (2002) 351–356.
- [42] T. Cierpicki, J.H. Bushweller, Charged gels as orienting media for measurement of residual dipolar couplings in soluble and integral membrane proteins, *J. Am. Chem. Soc.* 126 (2004) 16259–16266.

- [43] B. Luy, K. Kobzar, H. Kessler, An easy and scalable method for the partial alignment of organic molecules for measuring residual dipolar couplings, *Angew. Chem., Int. Ed.* 43 (2004) 1092–1094.
- [44] J.C. Freudenberger, S. Knör, K. Kobzar, D. Heckmann, T. Paululat, H. Kessler, B. Luy, Stretched polyvinylacetate-gels as NMR-alignment media for the measurement of residual dipolar couplings in polar organic solvents, *Angew. Chem., Int. Ed.* 44 (2005) 423–426.
- [45] P. Haberz, J. Farjon, C. Griesinger, A DMSO compatible orienting medium: towards the investigation of the stereochemistry of natural products, *Angew. Chem., Int. Ed.* 44 (2005) 427–429.
- [46] G. Kummerlöwe, J. Auernheimer, A. Lendlein, B. Luy, Stretched poly(acrylonitrile) as a scalable alignment medium for DMSO, *J. Am. Chem. Soc.* 129 (2007) 6080–6081.
- [47] R.R. Gil, C. Gayathri, N.V. Tsarevsky, K. Matyjaszewski, Stretched poly(methyl methacrylate) gel aligns small organic molecules in chloroform. Stereochemical analysis and diastereotopic proton NMR assignment in ludartin using residual dipolar couplings and  $^3J$  coupling constant analysis, *J. Org. Chem.* 73 (2008) 840–848.
- [48] B. Luy, K. Kobzar, S. Knör, D. Heckmann, J. Furrer, H. Kessler, Orientational properties of stretched poly(styrene) gels in various organic solvents and the suppression of its residual  $^1H$ -NMR signals, *J. Am. Chem. Soc.* 127 (2005) 6459–6465.
- [49] J. Klages, H. Kessler, S.J. Glaser, B. Luy, J-ONLY-TOCSY: efficient suppression of RDC-induced transfer in homonuclear TOCSY experiments using JESTER-1-derived multiple pulse sequences, *J. Magn. Reson.* 189 (2007) 217–227.
- [50] J. Courtieu, J.P. Bayle, B.M. Fung, Variable-angle sample-spinning NMR in liquid crystals, *Progr. NMR Spectrosc.* 26 (1994) 141–169.
- [51] C.M. Thiele, Scaling the alignment of small organic molecules in substituted polyglutamates by variable-angle sample spinning, *Angew. Chem., Int. Ed.* 44 (2005) 2787–2790.
- [52] A. Saupe, Kernresonanzen in kristallinen Flüssigkeiten und in kristallinflüssigen Lösungen I, *Z. Naturforsch.* A 19 (1964) 161–171.
- [53] J. Courtieu, D.W. Alderman, D.M. Grant, J.P. Bayle, Director dynamics and NMR applications of nematic liquid-crystals spinning at various angles from the magnetic field, *J. Chem. Phys.* 77 (1982) 723–730.
- [54] M. Zweckstetter, NMR: prediction of molecular alignment from structure using the PALES software, *Nat. Protoc.* 3 (2008) 679–690.
- [55] R.S. Prosser, S.A. Hunt, J.A. DiNatale, R.R. Vold, Magnetically aligned membrane model systems with positive order parameter: switching the sign of  $\sigma_{zz}$  with paramagnetic ions, *J. Am. Chem. Soc.* 118 (1996) 269–270.
- [56] K.P. Howard, S.J. Opella, High-resolution solid-state NMR spectra of integral membrane proteins reconstituted into magnetically oriented phospholipid bilayers, *J. Magn. Reson. B* 112 (1996) 91–94.
- [57] R.S. Prosser, J.S. Hwang, R.R. Vold, Magnetically aligned phospholipid bilayers with positive ordering: a new model membrane system, *Biophys. J.* 74 (1998) 2405–2418.
- [58] P.W. Kuchel, B.E. Chapman, N. Müller, W.A. Bubb, D.J. Philp, A.M. Torres, Apparatus for rapid adjustment of the degree of alignment of NMR samples in aqueous media: verification with residual quadrupolar splittings in  $^{23}Na$  and  $^{133}Cs$  spectra, *J. Magn. Reson.* 180 (2006) 256–265.
- [59] G. Kummerlöwe, F. Halbach, B. Laufer, B. Luy, Precise measurement of RDCs in water and DMSO based gels using a silicone rubber tube for tunable stretching, *The Open Spectrosc. J.* 2 (2008) 29–33.
- [60] C. Naumann, P.W. Kuchel, Prochiral and chiral resolution in  $^2H$  NMR spectra: solutes in stretched and compressed gelatin gels, *J. Phys. Chem. A* 112 (2008) 8659–8664.
- [61] G. Kummerlöwe, E.F. McCord, S.F. Cheatham, S. Niss, R.W. Schnell, B. Luy, Tunable alignment for all polymer gel/solvent combinations for the measurement of anisotropic NMR parameters, *Chem. Eur. J.* 16 (2010) 7087–7089.
- [62] C. Gayathri, N.V. Tsarevsky, R.R. Gil, Residual dipolar couplings (RDCs) analysis of small molecules made easy: fast and tuneable alignment by reversible compression/relaxation of reusable PMMA gels, *Chem. Eur. J.* 16 (2010) 3622–3626.
- [63] R. Ulrich, R.W. Glaser, A.S. Ulrich, Susceptibility corrections in solid state NMR experiments with oriented membrane samples. Part II: theory, *J. Magn. Reson.* 164 (2003) 115–127.
- [64] J.W. Emsley, J. Feeney, L.H. Sutcliffe, High Resolution Nuclear Magnetic Resonance Spectroscopy, Pergamon Press, Oxford, 1965. Vol. 1.
- [65] J.W. Emsley, J.C. Lindon, NMR Spectroscopy Using Liquid Crystal Solvents, Pergamon Press, Oxford, 1975.
- [66] E.E. Burnell, C.A. De Lange, Effects of interaction between molecular internal motion and reorientation on NMR of anisotropic liquids, *J. Magn. Reson.* 39 (1980) 461–480.
- [67] J.G. Snijders, C.A. De Lange, E.E. Burnell, Vibration-rotation coupling in anisotropic environments: NMR of methanes in liquid crystals, *J. Chem. Phys.* 77 (1982) 5386–5395.
- [68] J.G. Snijders, C.A. De Lange, E.E. Burnell, Vibration-rotation coupling in anisotropic environments. II. Quadrupolar couplings of methanes in liquid crystals, *J. Chem. Phys.* 79 (1983) 2964–2969.
- [69] C.A. de Lange, W.L. Meerts, A.C.J. Weber, E.E. Burnell, Scope and limitations of accurate structure determination of solutes dissolved in liquid crystals, *J. Chem. Phys. A* 114 (2010) 5878–5887.
- [70] L.C. Snyder, S. Meiboom, NMR of tetrahedral molecules in a nematic solvent, *J. Chem. Phys.* 44 (1966) 4057–4058.
- [71] R. Ader, A. Loewenstein, Nuclear magnetic resonance spectra of deuterated methanes and 2,2-dimethylpropane in nematic liquid crystals, *Mol. Phys.* 24 (1972) 455–457.
- [72] L.W. Reeves, A.S. Tracey, Studies of membrane processes. I. The  $NH_4^+$ ,  $ND_4^+$ ,  $ND_3H^+$ , and  $CH_3ND_3^+$  ions in equilibrium with an oriented electrical double layer, *J. Am. Chem. Soc.* 96 (1974) 365–369.
- [73] F. Fujiwara, L.W. Reeves, A.S. Tracey, Membrane processes. V. Distortion of tetrahedral ions in the electrical double layer of a model membrane, *J. Am. Chem. Soc.* 96 (1974) 5250–5251.
- [74] A. Enthart, J.C. Freudenberger, J. Furrer, H. Kessler, B. Luy, The CLIP/CLAP-HSQC: Pure absorptive spectra for the measurement of one-bond couplings, *J. Magn. Reson.* 192 (2008) 314–322.
- [75] T.E. Skinner, T.O. Reiss, B. Luy, N. Khaneja, S.J. Glaser, Application of optimal control theory to the design of broadband excitation pulses for high resolution NMR, *J. Magn. Reson.* 163 (2003) 8–15.
- [76] T.E. Skinner, T.O. Reiss, B. Luy, N. Khaneja, S.J. Glaser, Reducing the duration of broadband excitation pulses using optimal control with limited RF amplitude, *J. Magn. Reson.* 167 (2004) 68–74.
- [77] K. Kobzar, T.E. Skinner, N. Khaneja, S.J. Glaser, B. Luy, Exploring the limits of broadband excitation and inversion pulses, *J. Magn. Reson.* 170 (2004) 236–243.
- [78] B. Luy, K. Kobzar, T.E. Skinner, N. Khaneja, S.J. Glaser, Construction of universal rotations from point-to-point transformations, *J. Magn. Reson.* 176 (2005) 179–186.
- [79] K. Kobzar, T.E. Skinner, N. Khaneja, S.J. Glaser, B. Luy, Exploring the limits of broadband excitation and inversion pulses II: RF-power optimized pulses, *J. Magn. Reson.* 194 (2008) 58–66.
- [80] D.S. Garrett, R. Powers, A.M. Gronenborn, G.M. Clore, A common sense approach to peak picking two-, three- and four-dimensional spectra using automatic computer analysis of contour diagrams, *J. Magn. Reson.* 95 (1991) 214–220.